Sorptive removal of phenolic endocrine disruptors by functionalized biochar: competitive interaction mechanism, removal efficacy and application in wastewater

Mohammad Boshir Ahmed, John L Zhou*, Huu Hao Ngo, Md Abu Hasan Johir, Kireesan Sornalingam

School of Civil and Environmental Engineering, University of Technology Sydney, 15 Broadway, NSW 2007, Australia

Corresponding author. Tel: 61 2 95142023. Email: junliang.zhou@uts.edu.au

Abstract

Sorptive removal of six phenolic endocrine disrupting chemicals (EDCs) estrone (E1), 17β-estradiol (E2), estriol (E3), 17α-ethynylestradiol (EE2), bisphenol A (BPA) and 4-*tert*-butylphenol (4*t*BP) by functionalized biochar (fBC) through competitive interactions was investigated. EDC sorption was pH dependent with the maximum sorption at pH 3.0-3.5 due to hydrogen bonds and π-π interactions as the principal sorptive mechanism. Sorption isotherm of the EDCs was fitted to the Langmuir model. Sorption capacities and distribution coefficient values followed the order E1 > E2 ≥ EE2 > BPA > 4*t*BP > E3. The findings suggested that EDC sorption occurred mainly through pseudo-second order and external mass transfer diffusion processes, by forming H-bonds along with π-π electron-donor-acceptor (EDA) interactions at different pH. The complete removal of ~500 μg L^{-1} of each EDC from different water decreased in the order: deionised water > membrane bioreactor (MBR) sewage effluent > synthetic wastewater. The presence of sodium lauryl sulphonate and acacia gum in synthetic wastewater significantly suppressed sorption affinity of EDCs by 38-50%, hence requiring more fBC to maintain removal efficacy.

Keywords: Functionalized biochar; EDC; Competitive sorption; Hydrogen bond; Sewage effluent

1. Introduction

Endocrine disrupting chemicals (EDCs) can cause adverse effects due to exogenous endocrine disruption in the reproductive, sexual differentiation, neurological and immune systems even at low concentrations (ng L^{-1} to μg L^{-1}), and have attracted increasing attention [1-2]. Phenolic structure based compounds such as the natural estrogens 17β-estradiol (E2), estriol (E3) and estrone (E1), synthetic estrogen 17α-ethynylestradiol (EE2), and industrial compounds such as octylphenol, nonylphenol, 4-*tert*-butyl phenol (*4t*BP) and bisphenol A (BPA), are the most potent EDCs. EDCs are poorly removed in sewage treatment plants [2-5] and are a primary source of their discharge and occurrence in surface water, groundwater, seawater and sediment [4, 6]. EDCs are relatively hydrophobic organic compounds according to their octanol-water partition coefficient (K_{ow}) values and have only one pK_a value. The chemical structures and physicochemical properties of the EDCs are shown in **Fig. 1 and Table 1**, respectively**.**

Many separation processes such as coagulation, flocculation and precipitation have been used for the removal of EDCs from different water [3, 5]. Conventional biological processes such as activated sludge, constructed wetlands, bio-filtration have shown limited removal of EDCs [3, 5] while advanced treatment processes such as granular activated carbon, photolysis, photocatalysis, ferrate [4] free radical oxidation, Fenton oxidation, sonolysis, membrane separation, chlorination and ozonation have shown more satisfying results [3, 5, 7, 8]. Some hybrid systems such as membrane bioreactor (MBR) followed by ultrafiltration/nanofiltration/reverse osmosis, flocculation followed by activated sludge and ultrafiltration can also remove EDCs efficiently from water and wastewater [3, 9]. However, a major problem of hybrid systems is the high capital investment and operation cost. Physical separation processes such as activated carbon adsorption, membrane filtration and ion exchange normally show superior removal efficiencies of the EDC [10, 11]. Adsorption of EDCs on carbonaceous materials has been studied using activated carbon [12-14] black

carbon, single- or multi-walled carbon nanotubes (SWCNT, MWCNT) [15, 16] and biochar [4, 17, 18]. Biochar is a low-cost sorbent for the efficient removal of many hydrophilic and hydrophobic organic contaminants [19, 20]. Sorption of EDCs has also been studied using alumina, silica and hydrophobic medium [21].

So far, the sorption of EDCs has been studied using single compound, although there are reports on using membrane-based processes for mixture removal. Although carbonaceous materials such as CNT, graphene, activated carbon and biochar may have natural properties to sorb different organic contaminants simultaneously from water, such data, especially on EDCs, is scarce. Little is known about their sorptive behaviour, mechanism, affinities and distribution coefficient in the competitive mode using carbonaceous materials. Therefore, this study was focused on the competitive removal of six EDCs namely E1, E2, E3, EE2, BPA and *4t*BP using functionalized biochar (fBC). The objectives were to study (i) the competitive sorption of EDCs using fBC, (ii) the detailed mechanism of EDCs' sorption, (iii) the trend of EDCs' removal by fBC, and (iv) the removal efficiency of EDCs from synthetic wastewater and MBR sewage effluent for practical applications.

2. Experimental

2.1. Chemicals and fBC sorbent

E1 (99%), E2 (> 98%), E3 (> 97%), EE2 (98%), BPA (99%), and *4t*BP (99%), and organic solvents such as methanol, acetonitrile of HPLC grade were purchased from Sigma-Aldrich, Australia. Formic acid was of 99.9% purity. Potassium chloride (≥ 99.0%) and sodium chloride (≥ 99.5%) were of analytical grade. *Eucalyptus globulus* was donated by New Forest Asset Management Pty Ltd, Portland, Victoria, Australia.

First 30 g of *Eucalyptus globulus* wood particles (0.425-1.00 mm size) were pyrolyzed to obtain biochar at 400 ^{o}C under flowing nitrogen at 2.5 psi for 2 h. The biochar yield was 34.0-35.0%. The activation of biochar was carried out following a method described

previously [22]. Briefly, biochar was activated by soaking in 50% *ortho*phosphoric acid ($o$$H_3PO_4$) with the impregnation ratio 1:1 (w/v, taking $o$$H_3PO_4$ as 100%) for 3 h at 50 °C followed by heating at 600 °C for another 2 h. Prepared material was cooled in the reactor, washed several times with distilled water, and the pH was adjusted to ~7, followed by drying overnight at 100 °C. After activation, ~15-20% weight loss (activated burn off) was observed. Average particle size of activated biochar was in the range 75-600 µm. As the activated biochar was enriched with different functional groups such as –COOH, -OH, C=O and C=C on its surface, (based on X-ray Photoelectron Spectroscopy (XPS) characterization) the prepared activated biochar was termed as fBC.

2.2. EDCs sorption on fBC in different water

Competitive sorption experiments of EDCs on fBC were conducted in 50 mL glass vials with Teflon-lined screw caps at 25 ^{o}C in duplicate. EDCs were dissolved in methanol to prepare the stock solution of 1.0 g L^{-1}. The final methanol content in the sorption system was <0.5% (v/v) to avoid the co-solvent effect. To study the effect of pH, the interaction of pre-equilibrated fBC (20 mL of solution at the same solution pH) with EDC mixture in solution (25 mL) was carried out at different pH values (1.86, 3.1, 4.0, 5.1, 5.96, 7.85, 9.0 and 10.85) for 42 h at 25 ^{o}C. The initial concentration of each EDC in the mixture was adjusted to ~500 µg L^{-1}. Competitive sorption isotherm and kinetics experiments of EDCs in duplicate were also performed on an orbital shaker at 110 rpm, 25 ^{o}C for 48 h at pH ~3.0-3.25. Constant ionic strength was maintained using 0.01 M NaCl. The solid phase sorption (q_s, µg g^{-1}) and sorption distribution coefficient (K_d, L kg^{-1}) were calculated. The initial concentrations of each EDC were in the range ~250 µg L^{-1} to ~3000 µg L^{-1} in the mixture solution. The control experiments without sorbents were also performed. The sorbent dosage was selected for 15 to 95% sorption of each EDC at different concentrations. After equilibrium, the pH was measured and the solution was filtered through a 0.2 µm PTFE filter and analyzed by high-

performance liquid chromatography (HPLC). Raw biochar showed low removal efficiency hence, the discussion on the results obtained with unmodified biochar is not presented here.

The removal of EDCs spiked to synthetic wastewater and MBR effluent (collected from Central Park, Sydney, Australia) were also studied. The chemical composition of synthetic wastewater is as follows: peptone (2.37 mg L^{-1}), beef extract (1.8 mg L^{-1}), humic acid (4.2 mg L^{-1}), tannic acid (4.2 mg L^{-1}), sodium lignin sulphonate (2.4 mg L^{-1}), Na-lauryl sulphate (0.94 mg L^{-1}), acacia gum powder (4.37 mg L^{-1}), arabic acid (5.0 mg L^{-1}), ammonium sulphate (7.1 mg L^{-1}), K_2HPO_4 (7.0 mg L^{-1}) and $MgSO_4.3H_2O$ (0.71 mg L^{-1}) [23]. MBR effluent was filtered (1.2 μm) before being stored at 4 ^oC. MBR effluent and synthetic wastewaters were spiked with ~500 μg $L^{-1}$of each EDC in the mixture before interaction with fBC for 44 to 64 h at pH 3.0-3.25, (maximum sorption-based on the pH study) at 25 ^oC. Different dosages of fBC were used to study the removal of EDCs in competitive mode. The concentrations of the target EDCs in the MBR effluent were lower than the limit of detection (LOD), hence EDCs were spiked to MBR effluent. Synthetic wastewater and MBR effluent were used to examine the effect of different constitutes (organics and inorganics) present in these waters, on the removal of EDCs. The physicochemical properties of MBR sewage effluent and synthetic wastewater are listed in **Table S1**.

2.3. Characterization of fBC

Microscopic analysis of fBC before and after EDC sorption was carried out using scanning electron microscope (SEM) (Zeiss Evo-SEM). Brunauer-Emmett-Teller (BET) nitrogen adsorption-desorption isotherms and Barrett-Joyner-Halenda (BJH) method were used to calculate specific surface area and the porosity of fBC using a Micromeritics 3 FlexTM surface characterization analyzer at 77 K. The bulk elemental analysis (C, H, O, N, P) of fBC was determined using Oxford energy dispersive X-ray spectroscopy (EDS) and XPS (Thermo Scientific, UK). A Renishaw inVia Raman spectrometer (Gloucestershire, UK) equipped with

a Leica DMLB microscope (Wetzlar, Germany) and a 17 mW Renishaw helium neon laser source at 633 nm (with 50% of the laser intensity) with CCD array detector was used for Raman spectroscopy. The fBC was added to 0.01 M KCl solution at eight different pH values for 46 hours to measure its zeta potential (Nano-ZS, Malvern).

2.4. Analyses of EDCs

EDCs were analyzed by HPLC with an auto-sampler and a reverse-phase Zorbax Bonus RP C_{18} column (5.0 µm, 2.1 ×1.50 mm, Agilent Technologies), with an injection volume of 100 µL. Mobile phase "A" was composed of acetonitrile and formic acid (99.9: 0.1) while mobile phase "B" consisted of Milli-Q water and formic acid (99.9: 0.1). The elution used 40% of "A" and 60% of "B" at a flow rate of 0.4 mL min^{-1}, which was changed to 0.3 mL min^{-1} at 0.1 min and maintained until 9.0 min. After 9 min, the flow rate was changed to 0.2 mL min^{-1} and maintained up to 24 min. EDCs were analyzed with a UV detector at 285 nm and a fluorescence detector at 280 nm (excitation wavelength) and 310 nm (excitation wavelength). Fluorescence and UV wavelength were kept unchanged throughout the analysis. The method LOD for each EDC is given in **Table S2**.

2.5. Modeling of sorption kinetics, thermodynamics and isotherms

The sorption data were fitted to four kinetic models, namely pseudo first-order (PFO), pseudo second-order (PSO), the Weber–Morris intra-particle diffusion model (IDM) and the external mass transfer models as follow:

$$\text{PFO: } q_t = q_s(1 - e^{-K_1 t}) \quad (1)$$

$$\text{PSO: } q_t = \frac{K_2 q_s^2 t}{1 + K_2 q_s t} \quad (2)$$

$$\text{IDM: } q_t = K_i t^{\frac{1}{2}} + C \quad (3)$$

$$\left[\frac{d(C_t/C_o)}{dt}\right]_{t=0} = -\beta S \quad (4)$$

where K_i is the apparent diffusion rate constant (g μg^{-1} min$^{-1/2}$), q_t (μg g^{-1}) is the sorbed mass at time t, q_s (μg g^{-1}) is the equilibrium sorbent mass, K_1 (min^{-1}) is the PFO kinetic rate constant, K_2 (μg g^{-1} min^{-1}) is the PSO kinetic rate constant, and C is a constant (μg g^{-1}) that provides the thickness of the boundary layer [22].C_0 and C_t (μg L^{-1}) represent the concentrations of EDCs in solution at the beginning and at time t, respectively, β (cm min^{-1}) is the external mass transfer coefficient, and S (cm^{-1}) is the specific surface of fBC for external mass transfer. βS value was calculated from the slope of the C_t/C_0 versus t plot [5].

Gibbs free energy (ΔG°, kJ mol^{-1}) of EDCs sorption onto fBC at 25 ^{0}C was estimated with different concentrations using equation 5 [5]:

$$\Delta G^0 = -RT\ lnK_d \qquad (5)$$

where K_d (L kg^{-1}) is the apparent individual sorption distribution coefficient and can be defined by the ratio of sorbed EDC concentration (q_s, μg g^{-1}) to aqueous EDC concentration (C_w, μg L^{-1}), using equation 6:

$$K_d = 1000 \times \frac{q_s}{C_w} = 1000 \times \left(\frac{C_0 - C_w}{C_w}\right)\frac{V}{M} \qquad (6)$$

where V (L) is the solution volume, and M (g) is the sorbent mass.

The sorption data were also fitted to the Langmuir isotherm model which is represented below [23]:

$$\text{Langmuir model: } q_s = \frac{q_{max} K_L C_w}{1 + K_L C_w} \qquad (7)$$

where q_{max} is the maximum adsorption capacity (μg g^{-1}) and K_L is the Langmuir fitting parameter (L μg^{-1}). Parameters were estimated by nonlinear regression weighted by the dependent variable.

The sorption data obtained were used to calculate the total competitive sorption capacities using summarized Langmuir sorption (equations 8 and 9). Since all the competitive solutes interact and compete for the same sorption sites in fBC, the overall maximum sorption

capacity of fBC can be estimated by the additive contribution of each EDC's maximum sorption capacity [22].

The combined Langmuir model for six EDCs in competitive mode can be written as:

$$q_{total} = \frac{q_{max1}K_{L1}C_{S1}}{1+K_{L1}C_{S1}} + \frac{q_{max2}K_{L2}C_{S2}}{1+K_{L2}C_{S2}} + \frac{q_{max3}K_{L3}C_{S3}}{1+K_{L3}C_{S3}} + \frac{q_{max4}K_{L4}C_{S4}}{1+K_{L4}C_{S4}} + \frac{q_{max5}K_{L5}C_{S5}}{1+K_{L5}C_{S5}} + \frac{q_{max6}K_{L6}C_{S6}}{1+K_{L6}C_{S6}} \quad (8)$$

$$q_{max.(total)} = q_{max1} + q_{max2} + q_{max3} + q_{max4} + q_{max5} + q_{max6} \quad (9)$$

where q_{max1}, q_{max2}, q_{max3}, q_{max4}, q_{max5} and q_{max6} are the maximum Langmuir sorption capacity for E1, E2, E3, EE2, BPA and 4*t*BP, respectively. $q_{max.(\text{total})}$ is the total maximum Langmuir sorption capacity of the fBC for EDC mixtures, estimated by the summation of individual EDC's maximum sorption capacities.

3. Results and discussion

3.1. Characterization of fBC and EDCs

The structure of the carbon network in fBC was analysed by SEM, BET, XPS, FTIR and Raman spectra. SEM images of fBC after sorption experiments showed the development of flakes like structure on the fBC surface **(Fig. S1)**. **Fig. 2a** represents the nitrogen adsorption-desorption isotherm plot of fBC. This clearly indicates that isotherm plot was found to be type II isotherm. This isotherm features N_2-uptake increment up to a relative pressure of 0.5 then slightly reduced followed by an increment of N_2 adsorption (relative pressure up to 1.0) to reach a plateau. This result suggested the existence of mesopore (2-50 nm) and macrospore (> 50 nm) structure of fBC and the isotherm indicate unrestricted monolayer-multilayer adsorption [24, 25]. More clearly, the arrow (**in Fig.2a**) point, the beginning of the most linear middle section of the isotherm indicating the point at which monolayer coverage is complete and multilayer adsorption is about to begin. On the other hand, **Fig. 2b** shows the presence of mesopores (~2-50 nm) in fBC core structure which has been calculated from the adsorption branch of the isotherm by the BJH method [26]. Thus, the fBC mostly contained meso and macroporous structures and tis indicated that the activation method did not lead to the

development of microporous (< 2.0 nm) structures. Also, BET and Langmuir surface area were found to be 1.18 and 8.22 m^2 g^{-1}, respectively which was much lower than the reported values [27]. The BJH adsorption cumulative surface area of pores was also found to be 1.37 m^2g^{-1} and Dubinin-Astakov micropore surface area was found to be 0.52 m^2 g^{-1} (**Table S3**).

The Raman spectroscopy on fBC showed two characteristic peaks at 1341 and 1588 cm^{-1} (**Fig. 3**), which correspond to the D-band (disordered structure) and G-band (graphitic structures) of sp2-type carbon present in fBC [22, 28]. The relative band intensity ratio (I_G/I_D) is 1.04 (> 1), demonstrated the functionalization in fBC. It is important to note that Raman spectra of fBC featured a strong D-band, which illustrated a slightly more amorphous character (disordered) of the carbon in fBC owing to more oxygenated functional groups on its structure as functionalization of biochar was carried out using acid. D-band surface defect was possible by the introduction of other elements onto carbon structure during fBC preparation.

XPS results indicated that fBC was rich in different functional groups especially -C=C-, -C-O and -O-C=O [29]. Carbon (C1s) spectra of fBC showed that fBC surface was composed of aromatic carbon mostly -C=C- (284.8 eV) due to long chain arene unit, -C-O (286.3 eV), -C=O (287.8 eV), -COOH (289 eV) and π-π* (292.35 eV) due to functional groups (**Fig. 4a**). Also, fBC surface contained oxygenated and phosphorous-based functional groups/complexes. O1s spectra showed that oxygen content was mostly in the form of organic carbon (at 533.3 and 531.62 eV) (**Fig. 4b**) [30]. The P2p XPS spectrum of fBC showed a peak at 133.79 eV in the form pentavalent tetra coordinated phosphorus (PO_4 i.e. C-O-PO_3), as in polyphosphates and/or phosphates (**Fig. 4c**) [31]. The survey peaks showed the same results (**Fig. 4d**). The elemental composition of fBC was found to be 81.76% C, 13.32% O, 0.8% N and 2.3% P from XPS.

3.2. Effect of pH on competitive sorption of EDCs

The effect of pH for competitive EDCs' sorption against the solid-phase concentration of each EDC is shown in **Fig. 5a**. The sorption of individual EDC by fBC was highly pH dependent and was found to be moderate at very low pH ~1.85 (where fBC became positive). At this pH, q_s values of all EDCs were found to be low, which might be due to the repulsion between the positively charged fBC (zeta potential value was positive) and protonated EDCs (**Fig. 5b**). However, the EDC sorption at this pH might be due to the electron-donor-acceptor (EDA) interactions between oppositely charged arene units. Increase in pH from 1.85 to 3.5 increased the sorption capacity significantly. The q_{max} values of individual EDCs were ~4110, ~3356, ~3333, ~3350, ~2765 and ~2725 μg g^{-1} for E1, E2, EE2, BPA, *4t*BP and E3, respectively. The maximum sorption of EDCs could be due to EDA interactions along with strong hydrogen bonds formation [23, 32]. Further increase in pH from 3.5 to pH 5.0 led to a significant reduction of the sorption of each EDC. However, when pH was increased above 5.0, another high q_s value for EDC was observed at pH near 8.0. This was due to pK_a values (pH = pK_a + log[*salt*/*acid*]) of each EDC and surface hydroxyl groups on fBC, which were responsible for the formation of strong hydrogen bonds together with EDA interactions with the fBC surface functional groups. Further pH increases up to 10.85 caused a decrease of q_s value of each EDC because of the highly repulsion between the negatively charged fBC and the EDCs. Hydrogen bond formations, as well as EDA interactions, were not strong as solution pH was above the pK_a values of the EDCs. The E1 sorption was the highest among the EDCs studied. This was mainly due to the presence of C=O functional group on its structure which might help in EDA interactions. Thus, q_{max} values for all EDCs in mixture mode were obtained at pH 3.0-3.5 where significant EDC interactions with fBC occurred. Detailed sorption mechanism at different pH is discussed in section 3.5.

3.3. EDC sorption kinetics

The kinetics of the competitive sorption of EDCs onto fBC is shown in **Fig. 6**, with the apparent adsorption equilibrium reaching within ~42 h. Based on linear regression coefficient, the PSO model adequately described the kinetic data at 95% confidence level, compared to PFO kinetic model (data not tabulated for PFO model). From the PSO model, the q_s values were found to be 7642, 5439, 4403, 5469, 4749 and 4431 μg g^{-1} for E1, E2, E3, EE2, BPA and 4*t*BP, respectively (**Table 2**).

To further evaluate the competitive sorption, the kinetic data were fitted with external mass transfer and intraparticle diffusion models as they play a major role in sorption process (**Fig. 6, Table 2**). For intra-particle diffusion model, piecewise linear regression analysis of each EDC showed that q_t vs $t^{0.5}$ plots had three distinct regions. The first linear portion included the sorption period of 9.43 to 23.24 $min^{0.5}$ which represents external mass transfer and binding of EDCs by active sites on the outer surface of the fBC. The second linear portion included the sorption period of 23.24 to 40.24 $min^{0.5}$ represents intra-particle diffusion and binding of EDCs by active sites on macro and mesopores. The third linear portions included the period of 40.24 to 53.67 $min^{0.5}$, which denoted the establishment of the equilibrium [5]. The third step was very slow, thus, could not be treated as a rate-accelerating step. In addition, linear regression coefficient values were significant ($r^2 > 0.90$). The linear regression fittings for individual EDC did not pass through the origin, i.e. deviating from the origin or near saturation. This might be due to the difference in the mass transfer rate of the EDCs in the initial and final stages of sorption. From intercept (*C*) data it was found that the intra-particle diffusion was not the sole rate-limiting step [5]. The external mass transfer also played an important role in controlling the sorption rate. The regression coefficients ($r^2 > 0.950$) of all EDCs showed that the competitive sorption of EDCs could be represented by the external mass transfer model (**Fig. 6b**).

The Boyd plot (equation 10) was used to explore whether intra-particle and external mass transfer processes exerted any significant influence on the sorption rate of EDCs [5]:

$$B_t = -\ln\left(1 - \frac{q_t}{q_s}\right) - 0.4977 \quad (10)$$

From the Boyd plot, it can be observed that none of the sorption data lines pass thorough the origin (**Fig. 6c**), indicating that the external mass transfer governed the sorption of EDCs on fBC. This finding is consistent with the previous study for BPA sorption using MWCNT where the external mass transfer was solely responsible for the sorption of BPA [5]. Thus, the sorption kinetics of EDCs could be described by PSO and external mass transfer models.

3.4. Competitive sorption of EDCs and Gibbs free energy

The variations of solid phase concentration of EDCs with aqueous equilibrium concentration are represented in **Fig. 7**. The isotherm data for competitive sorption of EDCs were fitted with Langmuir isotherm model. The Langmuir q_{max} were found to be 7588, 5126, 4217, 5115, 4764 and 4567 μg $g^{-1}$for E1, E2, E3, EE2, BPA and *4t*BP, respectively with regression coefficient > 0.940 for all EDCs (**Table S4**). The total sorption capacity of fBC was found to be ~31375 μg g^{-1} based on the summarized Langmuir model for selected EDCs. Since the solutes competed for the same fBC surface during sorption, the solute (EDC) with the highest interactions led to the highest sorption. The competitive sorption affinities followed the order: E1 > E2 ≥ EE2 > BPA > *4t*BP > E3. The higher solid phase concentration of EDCs could be attributed to the functionalization of the biochar, which resulted in the formation of additional sorption sites with increased functional groups and an increase in specific surface area and micro pore volume [22]. The observed interactions were comparable with reports for sorption of various solutes by different carbon nanomaterials such as SWCNT, MWCNT and fullerene [15]. For example, carbon nanomaterials were applied for the sorption of BPA and EE2 (seperately) and it was observed that the solid phase concentrations (1×10^4 - 1×10^5 μg g^{-1}) were within the range observed in this study for competitive sorption, if the same initial EDC concentration was maintained [15]. This implies that mixture of EDCs did not have adverse effect on the sorption of individual EDC using fBC. In comparison, limestone sediment was

found less effective for the sorption interactions with BPA, E2, EE2, 4-*tert*-octylphenol and 4-n-nonylphenol, with the Freundlich constant values being significantly lower with prolonged interaction time than in this study [2]. Ying et al. [2] found the concentrations in sediment were 45, 70, 80 and 1750 μg kg^{-1} for BPA, E2, EE2, 4-*tert*-octylphenol, respectively. Similarly, lower Langmuir and Freundlich isotherm parameters were reported for BPA and EE2 interactions with sewage sludge [33]. Lorphensri et al. [21] also found EE2 removal using alumina, silica and a hydrophobic medium (porapak P) was significantly lower than in this study. Furthermore, there was a significant linear relationship between log K_d and log C_w ($r^2 > 0.98$) (**Fig. S3**). Increase in EDCs concentration reduced K_d value of each EDC which resulted in a decrease in removal efficiency. This was due to the gradual saturation of fBC surface at higher solute concentrations, leading to lower removal efficiencies.

The sorption spontaneity of EDCs at different concentrations (~250 to 3000 μg L^{-1}) onto fBC was examined and Gibbs free energy was calculated (**Table S5**). The ΔG^0 values ranged from -29.01 to -20.17, -26.57 to -19.01, -24.78 to -18.25, -25.77 to -18.86, -24.91 to -18.38, and -24.09 to -18.68 kJ $mole^{-1}$for E1, E2, E3, EE2, BPA and 4*t*BP, respectively, when each EDC concentration was increased from ~250 to 3000 μg L^{-1}. Thus, the negative ΔG^0 values showed the spontaneous nature of the sorption of EDCs onto fBC.

3.5. Competitive sorption mechanism

Interaction mechanism of each EDC with fBC can be explained based on experimental findings. fBC core structure consisted of meso- and macro-pores. The BET surface area and Dubinin-Astakov micropore surface area were 1.183 and 0.516 m^2 g^{-1}, respectively. BJH adsorption average pore diameter of fBC was ~8.0 nm which might enough for diffusion of EDCs onto fBC pores as the apparent molecular size of EDCs molecules was well below the average pore diameter of fBC (**Table 1**). However, from the kinetics study, it was found that both external mass transfer (sorption by active sites) and PSO (multilayer sorption) model

parameters satisfactory described sorption kinetic behaviour of EDCs on fBC, suggesting the role of surface functional groups present in fBC for EDCs sorption. The mechanism of EDCs sorption by surface functional groups of fBC is described below at different pH conditions.

Fig. 3 shows the Raman spectra after sorption of a mixture of EDCs in competitive mode. The graphitic structure G-bands (mainly -C=C-arene unit) intensity was reduced significantly after sorption of EDCs in competitive mode. It suggested π-π interactions among EDCs and fBC (mostly in arene unit of biochar), whereas surface defect D band (due to defect structure) was decreased greatly indicating the role of surface functional groups. These functional groups were mostly oxygenated as confirmed by the XPS data. The decreases of peak intensity clearly suggested that hydrogen bond formation with the fBC functional groups as well as with EDCs' functional groups were the main interaction mechanisms. The I_G/I_D ratio also decreased significantly indicating strong interactions between fBC surface functional groups and EDCs.

Varying pH can affect the protonation-deprotonation transition of functional groups on any carbonaceous materials and change the chemical speciation for ionisable organic compounds [5]. The zeta potential values of fBC suspension in aqueous solution at various pH were determined, and point of zero charge was found to be 2.2 (**Fig. 5b**). Lower sorption of any compound at this pH was highly expected. At pH below 2.2, the zeta potential value of fBC was found to be the positive indicating surface of fBC was protonated under highly acidic conditions. EDCs molecules might also become protonated at pH 1.85 (e.g. due to hydroxyl or ketonic groups in EDCs). Hence, electrostatic repulsion of the same charge of quadruples might lead to lower sorption of EDCs at pH < 2.2. However, highly acidic condition (at pH 1.85) was still favourable to sorb EDCs by fBC to some extent. The EDA interactions can explain the sorption of EDCs at this pH. Chemical structures of all EDCs contain at least one hydroxyl group in arene unit, i.e. phenolic group, and due to resonance-effect of arene unit, nearby carbon atoms in hydroxyl group (in arene unit) could act as π-

electron donor site (**Figs 1 and S4**). Meanwhile, fBC consisted of ketonic and carboxylic -C=O functional groups in its arene units (as confirmed by XPS) which might act as π-electron acceptor site for the interactions (due to resonance) and the graphene unit in fBC can act as a π-electron donor site. Thus, stronger EDA interactions (from C=O and COOH as π-electron acceptor while EDCs as a π-electron donor) would be the main reason for the sorption of all EDCs at this pH (**Fig. S4**). The π-π electron-donor-donor (EDD) interactions between phenolic –OH of EDCs and surface –OH group and graphene unit of fBC are not significant, and considered weaker than EDA interactions. Thus, EDD interactions at very low pH can be excluded. The interactions of fBC and EDCs can also be predicted from pH shift tests before and after adsorption experiments. The variation of solution pH is shown in **Fig. 5b**. The equilibrium pH slightly increased after sorption (from 1.86 to 2.09) indicating either release of hydroxyl ions or consumption of proton either by fBC or EDCs. Moreover, hydroxyl ions might exchange proton in the solution for neutralization leading to increase the solution pH. However, proton exchange for fBC at pH ~1.85 is not favourable for –C=O, -COOH and -OH groups as their pK_a values are higher. Hence, surface –OH groups or quaternary nitrogen groups (tiny fraction) of fBC as well as EDCs functional groups such as –OH and -CH might form hydrogen bond along with EDA interactions, i.e. excess hydrogen ions took part in hydrogen bond formations hence equilibrium pH was increased. Therefore, sorption at pH ~1.85 was observed due to EDA interactions and hydrogen bond formations.

The maximum solid phase concentration and K_d values of all EDCs were observed at pH 3.0-3.5 (**Fig. 5a**), and the main reason might be due to the formation of strong hydrogen bonds and strong EDA interactions. Based on the pH shift study, equilibrium pH shifted slightly to higher pH (pH 3.10-4.0 to 3.25-4.18). The increase in equilibrium pH indicated hydroxyl groups released into solution, which was more significant in the control experiments than sorption experiment (**Fig. 5b**). Although the pH shift seemed less significant in the sorption experiments, the release of protons from fBC functional groups (e.g. –COOH) and

then forming strong hydrogen bonds (-COOH in fBC and phenolic –OH in EDCs) might be the main reason for resisting equilibrium pH to decrease (**Fig. 5b**). Such hydrogen bonds can be proposed as charge assisted hydrogen bonds (CAHB), i.e. fBC-CO^-/COO^-….H^+…O^--EDCs. Stronger hydrogen bonds might be possible with –OH groups and –CH groups in EDCs with fBC surface functional groups (e.g.–COOH, -OH, C=O, C≡N groups and C-O-PO_3 complex). However, EDA interactions could be considered the main sorption mechanism. The surface –COOH has pK_a value of ~3.0-5.0 [22, 34, 35]. Functional groups -COOH and C=O could act as strong π-electron acceptor while the phenolic group in EDCs and graphene unit of fBC could act as π-electron donor site (**Fig. S4**). Thus, stronger EDA interactions could be the main sorption mechanism. EDD interactions might not be significant as graphene surface could act as π-electron donor site as well as EDCs could act as π-electron donor. Hence, EDA interactions were the main mechanism for higher sorption of EDCs with additional contribution from the CAHB formations. Zhang et al. [5] studied the separation of BPA using MWCNT and proposed the π-π stacking interactions between the bulk π-system of MWCNT surface and BPA molecule in a wide pH range of 4.0 to 10.0 [5]. They also mentioned that MWCNT could function as hydrogen bond donor to form hydrogen bonds with –OH functional groups on BPA. However, they did not mention any specific group in MWCNT responsible for π-π stacking interactions, while our observations indicated that π-π stacking interactions (EDA) only came from the surface –COOH/C=O and -C=C- groups. Also, Jung et al. [11] studied the adsorption of emerging contaminants such as EE2, BPA, sulfamethoxazole, atrazine, carbamazepine, diclofenac and ibuprofen using activated biochar at different pH (3.5, 7.0, 10.5) and suggested that maximum adsorption was mainly due to π-π interactions. Therefore, maximum interactions might be due to the formation of negative CAHB as well as strong hydrogen bonds, with the main contribution from EDA interactions leading to the higher interaction of EDCs with fBC.

With the increase in pH from 3.0 to 5.0, the solid phase concentration of all EDCs decreased. When pH was increased from 5.0 to 8.0, another peak interaction value for all EDCs was found although not as high as at pH ~3.0-3.5. All the EDCs have one pK_a value. So, near pH 8-9 proton release from any EDC is highly possible as pH= pK_a+ log [salt/acid]. On the other hand, any carbonaceous surface –OH group has pK_a value of ~8.0-10.0 [5, 34]. Proton exchange by EDCs molecules was calculated and found their ΔG^o values were favourable for proton exchange in solution at this condition (**Table 3**). Thus, negatively charged surfaces (zeta potential was negative, and EDCs released a proton and became negative sites) could repulse each other causing minimum interactions. However, at pH ~8.0 high interactions were observed for all EDCs. This might be due to the formation of strong hydrogen bonds among hydroxyl group of EDC and fBC surface –OH groups, firstly, releasing the hydrogen ion from fBC or EDC hydroxyl group to neutralize –OH from water molecule (splitting of water molecule) leading to shift in the equilibrium pH toward more acidic region to form CAHB (fBC-O^-….H^+… O-EDCs) (**Fig. 5b**) [35-37]. In comparison with control experimental equilibrium pH, the change of equilibrium pH was also significant indicating the release of protons from surface –OH groups of fBC (**Fig. 5b**). The π-π EDA interactions could also play an important role under this condition. However, EDA interaction might only come from fBC surface -C=O groups (π-electron acceptor), graphene unit of fBC (as a π-electron donor) and EDCs (as a π-electron donor) whereas, EDA interactions might not be effective for the surface carboxylic group (pK_a value is near pH 3.0-5.0) (**Fig. S 4**) [35-37]. EDD interactions might be less effective. Furthermore, at pH > 9.0, each EDC may exist as an anion, and the sorption was significantly impeded due to the electrostatic repulsive force between negatively charged fBC surface and EDCs anions. The ionized forms of EDCs were the predominant fraction at pH > pK_a, and the hydrogen bonds and hydrophobic interactions between fBC and each ionized EDC were much weaker than those between fBC and non-ionized EDCs. Besides, both EDC and fBC were negatively charged, and the electrostatic

repulsion between them can also weaken their adsorption to some extent at pH > 10. Hence, lower sorption at pH above 9.0 was observed. In addition, the pH shift result was not significant at pH 10.85 indicating the insignificant role of the hydrogen bond formation.

3.6. EDC removal from sewage effluent vs. synthetic wastewater

When fBC was applied to remove a mixture of EDCs from MBR sewage effluent (spiked at 508.4, 525.9, 532.9, 534.5, 465.8, 460.5 μg L^{-1} of E3, BPA, *4t*BP, E2, E1 and EE2, respectively) at pH 3.0-3.25 and 25 ^{o}C, pronounced differences were observed for different EDCs in terms of their complete sorption onto fBC (**Fig. 8**). Using fBC dosage of 100, 200 and 300 mg L^{-1} was not enough to remove the EDCs in mixture mode at the specified concentration of each EDC. Better removal results were obtained with a higher dose of 400 mg L^{-1} of fBC, achieving ~97% removal of E3 and *4t*BP. Although the complete removal of E1 (460.5 μg L^{-1}) was found at 300 mg L^{-1} of fBC in competitive mode, the complete removal of EE2, E2 and BPA was obtained only at 400 mg L^{-1} of fBC. The results indicated that sorption interactions of EDCs with fBC were very efficient and dosage above 400 mg L^{-1} of fBC can remove the EDCs completely in competitive mode from the MBR effluent. The removal trend was the same as obtained from isotherm, pH effect and sorption affinity data as E1 > E2 > EE2 > BPA > 4*t*BP > E3. However, MBR effluent was found to have a slightly negative influence on the overall removal of EDCs than deionized water and thus required an extra dosage of fBC. The main reason might be the presence of different species in MBR effluent that may compete for the fBC surface and might block the surface functional groups of fBC, leading to reduced sorption of EDCs onto fBC surface than in deionized water.

Synthetic wastewater also contains a mixture of different organic acids, organic compounds and inorganic salts (**Table S1**). The removal of EDCs from synthetic wastewater was carried out at various dosages of fBC and residual concentration of each EDC was measured after 46, 50 and 64 h. Each EDC was spiked in synthetic wastewater (~500 μg L^{-1})

with individual concentration (measured after spiking) of 461.3, 486.0, 498.7, 497.0, 465.9, 460.4 μg L^{-1} of E3, BPA, 4*t*BP, E2, E1 and EE2, respectively. The fBC dosage, residual concentrations and percentage removal of each EDC in mixture mode are given in **Table 4**. Approximately 94.2% of E3 was removed in 46 h, with 555 μg L^{-1} of fBC; when sorption time was increased to 64 h, the removal reached 100%. Similarly, complete removal of BPA was obtained within 50 h at 445 mg $L^{-1}$of fBC dosage. This result indicates that BPA can be removed at any dosage above 445 mg L^{-1} of fBC from a mixture ~500 μg L^{-1} of each EDC. A similar result was obtained for 4*t*BP. Slightly long duration (~64 h) was needed for 100% removal of E1, E2 and EE2 at fBC dosage of 445 mg L^{-1}. The interactions of EDCs with fBC in synthetic wastewater were found to have an adverse influence on the overall removal of EDCs than with deionized water or MBR effluent. **Table S1** shows that MBR effluent composition is more complicated than synthetic wastewater. The main reason for slow interactions arose from different organics in synthetic wastewater (e.g. Na-laryl sulphate, beef extract, sodium lignin sulfonate, humic acid, tannic acid) and from inorganic sulfates and bi-phosphate. To shed light, separate competitive sorption experiments using fBC was conducted in the presence of Na-laryl sulphate and acacia gum powder (same concentration as used in synthetic wastewater), and it was observed that EDC sorption was significantly suppressed by 38-50%. Also, control experiments in the absence fBC showed that there was no loss of each EDC. Thus, the presence of Na-laryl sulphate and acacia gum powder in synthetic wastewater was the main cause for the reduced sorption of EDCs. Hence, an increased fBC dosage (>555 mg L^{-1}) is needed to ensure sufficient removal of EDC mixture from synthetic wastewater.

4. Conclusions

In this work fBC with enhanced functional groups, specific surface area, and meso- and macro-poreswas successfully prepared for the removal of EDC mixture from water and wastewater. The sorptive removal of EDCs by fBC through competitive interactions reached

equilibrium within 42 h, with the external mass transfer diffusion process as the rate-limiting step. PSO well modeled the sorption kinetics. EDC sorption was highly pH dependent, with the maximum sorption occurring at pH ~3.0-3.5. The sorption equilibrium followed the Langmuir isotherm model, suggesting monolayer coverage. In term of sorption mechanism, EDC sorption mainly occurred through π-π EDA interactions and by forming different hydrogen bonds. Overall, the sorption capacity and distribution coefficient values decreased as E1 > E2 ≥ EE2 > BPA > *4t*BP > E3 due to the difference in the EDCs' hydrophobicity. Water composition had a pronounced effect on EDC removal, as shown by the highest removal in deionised water, followed by MBR sewage effluent, and finally synthetic wastewater. The presence of sodium lauryl sulphonate and acacia gum in synthetic wastewater caused a significant reduction in the competitive sorption of EDCs on fBC. Thus, fBC can be successfully applied for the removal of EDC mixtures from water and wastewater, although appropriate pre-treatment may be required to remove the interfering substances such as certain surfactants.

Acknowledgements

We thank New Forest Asset Management Pty Ltd, Victoria, Australia for *Eucalyptus globulus* wood samples and Flow Systems for MBR effluent from the Central Park, Sydney.

References

[1] K. Sornalingam, A. McDonagh, J.L. Zhou, Photodegradation of estrogenic endocrine disrupting steroidal hormones in aqueous systems: Progress and future challenges, Sci. Total Environ. 550 (2016) 209-224.

[2] G.G. Ying, R.S. Kookana, P. Dillon, Sorption and degradation of selected five endocrine disrupting chemicals in aquifer material, Water Res. 37 (2003) 3785-3791.

[3] M.B. Ahmed, J.L. Zhou, H.H. Ngo, W. Guo, N.S. Thomaidis, J. Xu, Progress in the biological and chemical treatment technologies for emerging contaminant removal from wastewater: a critical review, J. Hazard. Mater. 323 (2017) 274-298.

[4] J.Q. Jiang, Q. Yin, J.L. Zhou, P. Pearce, Occurrence and treatment trials of endocrine disrupting chemicals (EDCs) in wastewaters. Chemosphere 61 (2005) 544-550.

[5] L. Zhang, P. Fang, L. Yang, J. Zhang, X. Wang, Rapid method for the separation and recovery of endocrine-disrupting compound bisphenol AP from wastewater, Langmuir 29(2013) 3968-3975.

[6] K. Maskaoui, J.L. Zhou, Colloids as a sink for certain pharmaceuticals in the aquatic environment. Environ. Sci. Pollut. Res.17 (2010) 898-907.

[7] S. Esplugas, D.M. Bila, L.G.T. Krause, M. Dezotti, Ozonation and advanced oxidation technologies to remove endocrine disrupting chemicals (EDCs) and pharmaceuticals and personal care products (PPCPs) in water effluents, J. Hazard. Mater. 149 (2007) 631-642.

[8] A. Zhang, J. Wang, Y. Li, Performance of calcium peroxide for removal of endocrine-disrupting compounds in waste activated sludge and promotion of sludge solubilization, Water Res. 71 (2015) 125-139.

[9] R. Rosal, A. Rodríguez, J.A. Perdigón-Melón, A. Petre, E. García-Calvo, M.J. Gómez, A. Agüera, A.R. Fernández-Alba, Occurrence of emerging pollutants in urban wastewater and their removal through biological treatment followed by ozonation, Water Res. 44 (2010) 578-588.

[10] D.P. Grover, J.L. Zhou, P. Frickers, J.W. Readman, Improved removal of estrogenic and pharmaceutical compounds in sewage effluent by full scale granular activated carbon: impact on receiving river water, J. Hazard. Mater. 185 (2011) 1005-1011.

[11] C. Jung, J. Park, K.H. Lim, S. Park, J. Heo, N. Her, J. Oh, S. Yun, Y. Yoon, Adsorption of selected endocrine disrupting compounds and pharmaceuticals on activated biochars, J. Hazard. Mater. 263 (2013) 702-710.

[12] A.M. Redding, F.S. Cannon, S.A. Snyder, B.J. Vanderford, A QSAR-like analysis of the adsorption of endocrine disrupting compounds, pharmaceuticals, and personal care products on modified activated carbons, Water Res. 43 (2009) 3849-3861.

[13] Z. Yu, S. Peldszus, P.M. Huck, Adsorption characteristics of selected pharmaceuticals and an endocrine disrupting compound—naproxen, carbamazepine and nonylphenol—on activated carbon, Water Res. 42 (2008) 2873-2882.

[14] C. Zhang, C. Lai, G. Zeng, D. Huang, C.Yang, Y. Wang, Y. Zhou, M. Cheng, Efficacy of carbonaceous nanocomposites for sorbing ionizable antibiotic sulfamethazine from aqueous solution, Water Res. 95 (2016) 103-112.

[15] B. Pan, D. Lin, H. Mashayekhi, B. Xing, Adsorption and hysteresis of bisphenol A and 17α-ethinyl estradiol on carbon nanomaterials, Environ. Sci. Technol. 42 (2008) 5480-5485.

[16] L. Zhang, F. Pan, X. Liu, L. Yang, X. Jiang, J. Yang, W. Shi, Multi-walled carbon nanotubes as sorbent for recovery of endocrine disrupting compound-bisphenol F from wastewater, Chem. Eng. J. 218 (2013) 238-246.

[17] C. Jung, L.K. Boateng, J.R. Flora, J. Oh, M.C. Braswell, A. Son, Y. Yoon, Competitive adsorption of selected non-steroidal anti-inflammatory drugs on activated biochars: Experimental and molecular modeling study, Chem. Eng. J. 264 (2015) 1-9.

[18] M.B. Ahmed, J.L. Zhou, H.H. Ngo, W. Guo, M. Chen, Progress in the preparation and application of modified biochar for improved contaminant removal from water and wastewater, Bioresour. Technol. 214 (2016) 836-851.

[19] M.B. Ahmed, J.L. Zhou, H.H. Ngo, W. Guo , Insight into biochar properties and its cost analysis, Biomass Bioenerg. 84 (2016) 76-86.

[20] M.B. Ahmed, J.L. Zhou, H.H. Ngo, W. Guo, Adsorptive removal of antibiotics from water and wastewater: Progress and challenges, Sci. Total Environ. 532 (2015) 112-126.

[21] O. Lorphensri, J. Intravijit, D.A. Sabatini, T.C. Kibbey, K. Osathaphan, C. Saiwan, Sorption of acetaminophen, 17α-ethynyl estradiol, nalidixic acid, and norfloxacin to silica, alumina, and a hydrophobic medium, Water Res. 40 (2003) 1481-1491.

[22] M.B. Ahmed, J.L. Zhou, H.H. Ngo, W. Guo, M.A.H.Johir, K. Sornalingam, Single and competitive sorption properties and mechanism of functionalized biochar for removing sulfonamide antibiotics from water, Chem. Eng. J. 311 (2017) 348-358.

[23] M.B. Ahmed, J.L. Zhou, H.H. Ngo, W. Guo, M.A.H.Johir, D. Belhaj, Competitive sorption affinity of sulfonamides and chloramphenicol antibiotics toward functionalized biochar for water and wastewater treatment, Bioresour. Technol. 238 (2017) 306-312.

[24] Z.A. Alothman, A review: fundamental aspects of silicate mesoporous materials, Materials 5 (2012) 2874-2902.

[25] M. Khalfaoui, S. Knani, M.A. Hachicha, A.B. Lamine, New theoretical expressions for the five adsorption type isotherms classified by BET based on statistical physics treatment, J. Colloid Interface Sci. 263 (2003) 350-356.

[26] S. Storck, H. Bretinger, W. F. Maier, Characterization of micro-and mesoporous solids by physisorption methods and pore-size analysis, Appl. Catal. A: General 174 (1998) 137-146.

[27] X. Dong, J. Fu, X. Xiong, C. Chen, Preparation of hydrophilic mesoporous carbon and its application in dye adsorption, Mater. Let. 65 (2011) 2486-2488.

[28] B. Peng, L. Chen, C. Que, K. Yang, F. Deng, X. Deng, G. Shi, G. Xu, M. Wu, Adsorption of antibiotics on graphene and biochar in aqueous solutions induced by π-π interactions, Sci. Rep. 6 (2016).

[29] T. Okpalugo, P. Papakonstantinou, H. Murphy, J. McLaughlin, N. Brown, High resolution XPS characterization of chemical functionalised MWCNTs and SWCNTs, Carbon 43 (2005) 153-161.

[30] V. Datsyuk, M. Kalyva, K. Papagelis, J. Parthenios, D. Tasis, A. Siokou, I. Kallitsis, C. Galiotis, Chemical oxidation of multiwalled carbon nanotubes, Carbon 46 (2008) 833-840.

[31] A.M. Puziy, O.I. Poddubnaya, R.P. Socha, J. Gurgul, M. Wisniewski, XPS and NMR studies of phosphoric acid activated carbons, Carbon 46 (2008) 2113-2123.

[32] M.B. Ahmed, J.L. Zhou, H.H. Ngo, W. Guo, M.A.H. Johir, K. Sornalingam, D. Belhaj, M. Kallel, Nano-Fe^0immobilized onto functionalized biochar gaining excellent stability during sorption and reduction of chloramphenicol via transforming to reusable magnetic composite, Chem. Eng. J. 322 (2017) 571-581.

[33] B. Banihashemi, R. L. Droste, Sorption–desorption and biosorption of bisphenol A, triclosan, and 17α-ethinylestradiol to sewage sludge, Sci. Total Environ. 487 (2014) 813-821.

[34] P. Gilli, L. Pretto, V. Bertolasi, G. Gilli, Predicting hydrogen-bond strengths from acid–base molecular properties. The pK_a slide rule: toward the solution of a long-lasting problem, Acc. Chem. Res. 42 (2008) 33-44.

[35] J. Ni, J.J. Pignatello, B. Xing, Adsorption of aromatic carboxylate ions to black carbon (biochar) is accompanied by proton exchange with water, Environ. Sci. Technol. 45 (2011) 9240-9248.

[36] M. Teixidó, J.J. Pignatello, J.L. Beltrán, M. Granados, J. Peccia, Speciation of the ionizable antibiotic sulfamethazine on black carbon (biochar). Environ. Sci. Technol. 45 (2011) 10020.

[37] C. Lattao, X.Y. Cao, J.D. Mao, K. Schmidtrohr, J.J. Pignatello, Influence of molecular structure and adsorbent properties on sorption of organic compounds to a temperature series of wood chars. Environ. Sci. Technol. 48 (2014) 4790-4798.

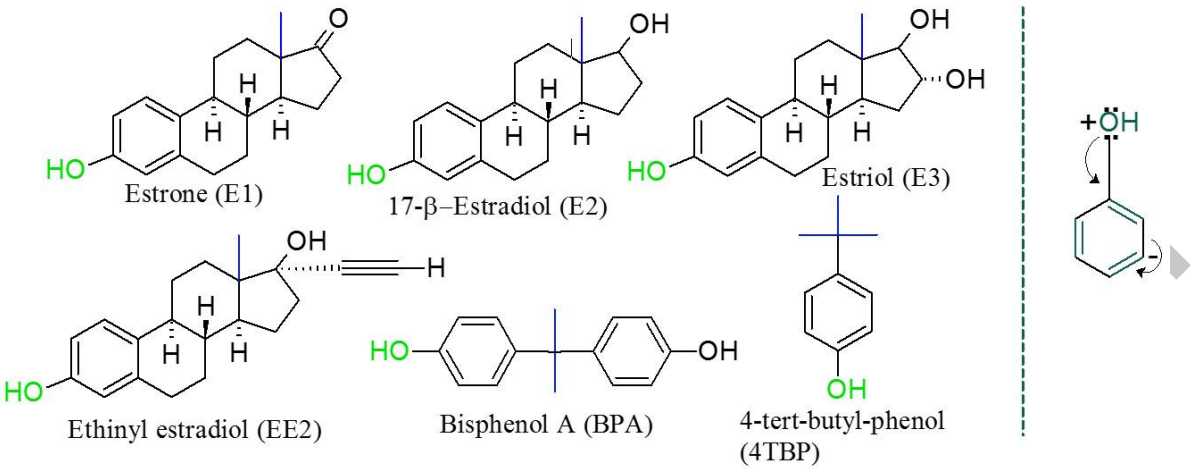

Fig. 1. Chemical structures of EDCs and resonance form of phenolic group in EDCs.

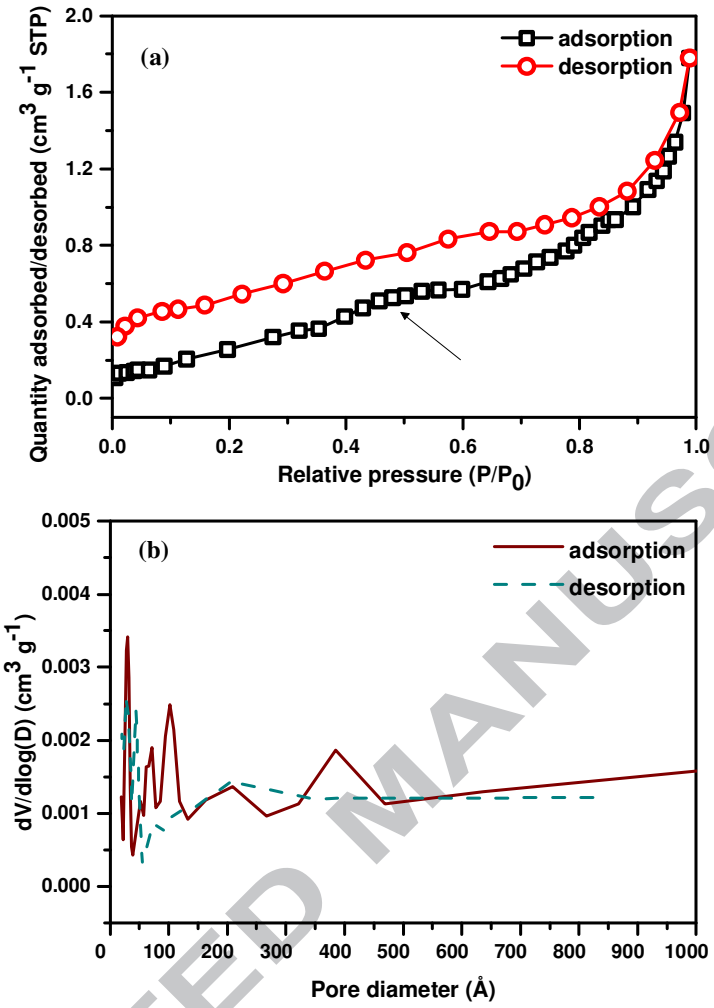

Fig. 2. Nitrogen adsorption-desorption isotherm for fBC: Barret-Joyner-Halenda (BJH) surface/ volume mesopore analysis (a), and cumulative pore size distribution (b).

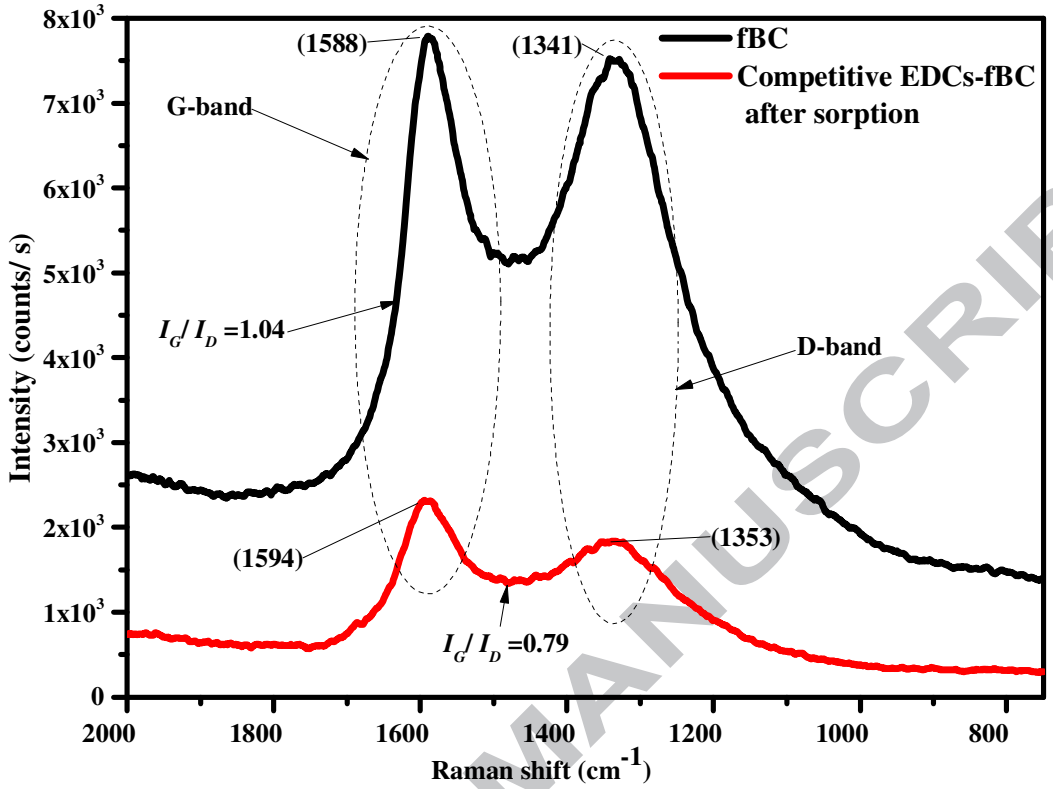

Fig. 3. Raman spectra for fBC before and after sorption experiments. Raman shifts measurement was carried out using Renishaw inVia Raman spectrometer equipped with a 17 mW Renishaw Helium-Neon Laser 633 nm and CCD array detector at 50% laser intensity.

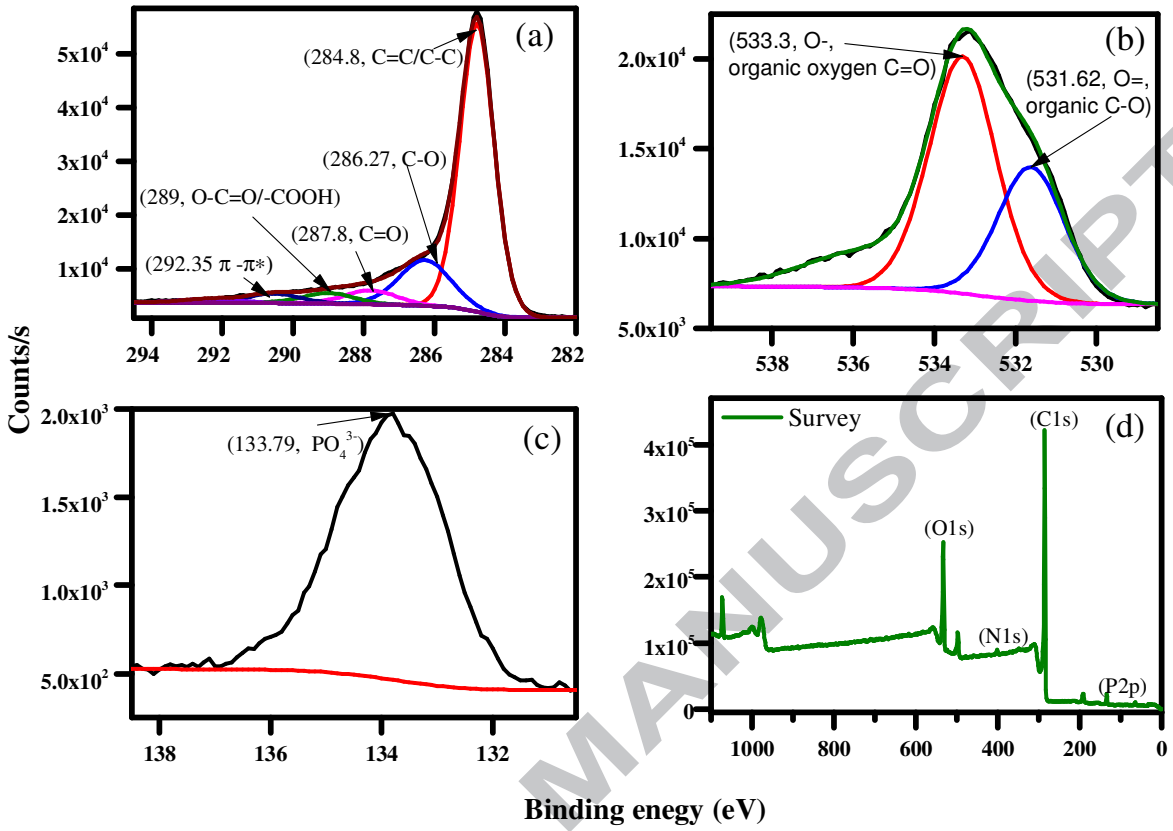

Fig. 4. XPS analysis of fBC. Spectra were obtained by plotting counts against binding energy in a wide scan for C1s (a), O1s (b), P 2p(c) and overall survey (d).

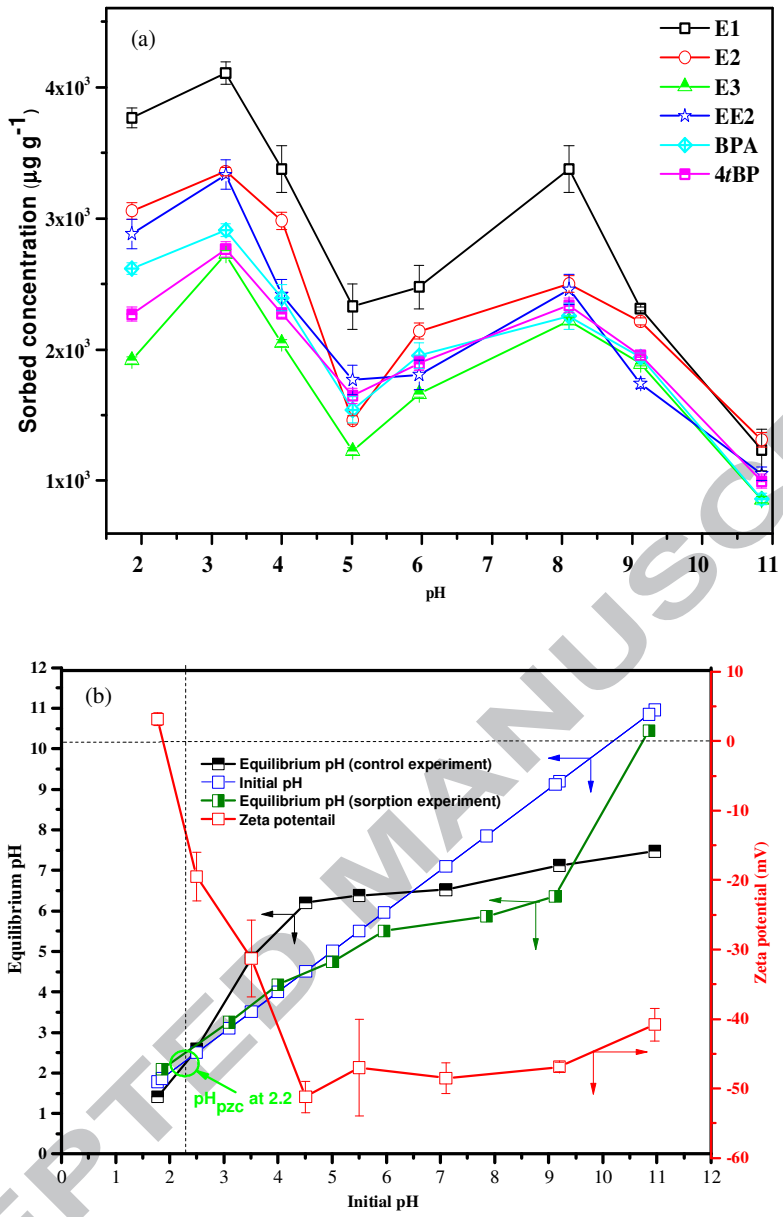

Fig. 5. Effect of pH on solid phase concentration (µg g^{-1}) during EDCs sorption in competitive mode using fBC at a dosage of 80 mg L^{-1} at 25 ^{o}C (a). Zeta potential values of fBC using 0.01 M KCl solution at different pH with fBC dosage of 400 mg L^{-1} together with initial and equilibrium pH values (b).

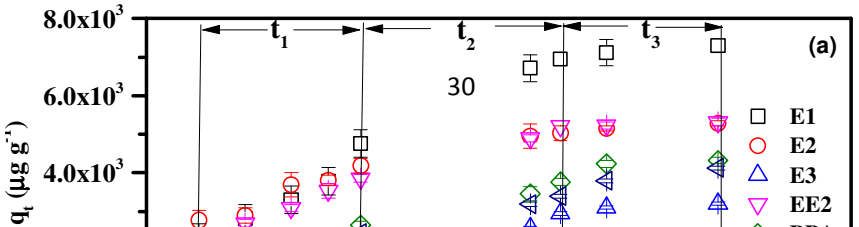

Fig. 6. Kinetic model fit for EDCs adsorption on fBC at 25 ^{o}C. (a) Weber-Morris plots, (b) external mass transfer plots, and (c) Boyd plots.

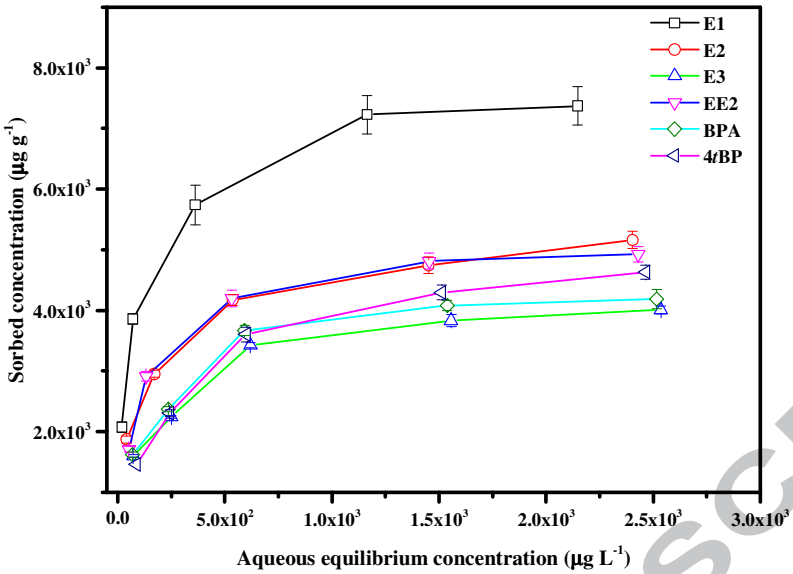

Fig. 7. Solid phase concentration vs. aqueous concentration at equilibrium for the sorption of EDCs using 100 mg L^{-1} of fBC at 25 ^{o}C.

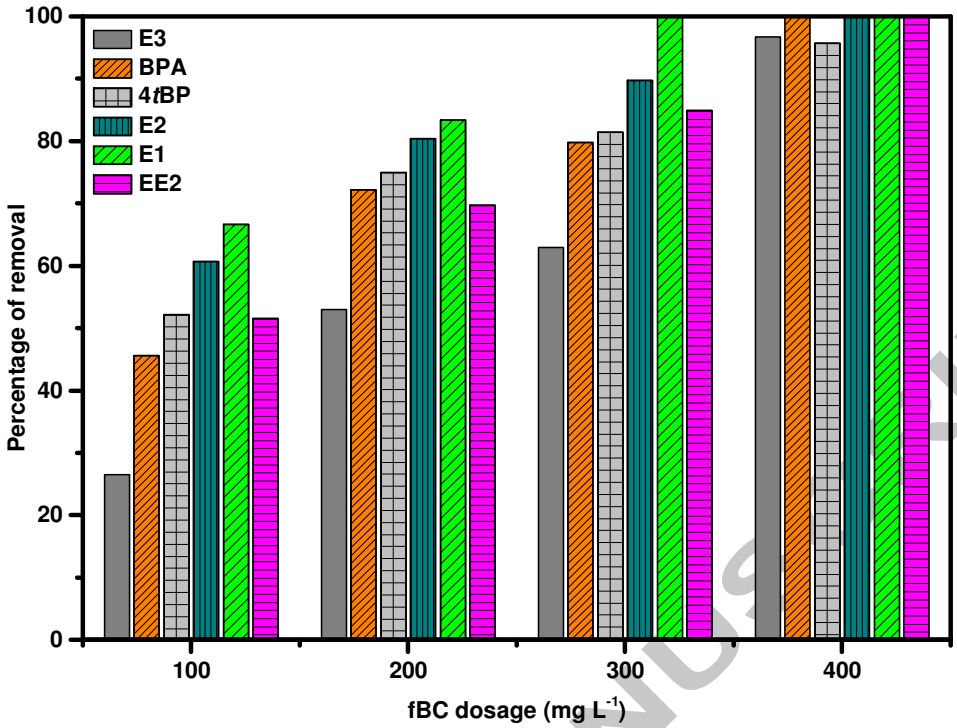

Fig. 8. Sorption of EDCs in mixture mode with initial concentration of each EDC at ~500 µg L^{-1} from MBR sewage effluent at different dosages of fBC at pH 3.0-3.25, 25 °C.

Table 1. Physicochemical properties of the target EDCs.

mpound	Molar mass (g mol^{-1})	Molar volume (cm^3 mol^{-1})	Molar density (g cm^{-3})	Volume of molecule (cm^3)	*log* K_{ow}	*log* K_{oc}	pK_a	Solubility in water (mg L^{-1})	Reference
	270.37	232.1 ± 3.0	1.164 ± 0.06	3.85×10^{-22}	3.13-3.43	3.1-3.5	10.34±0.05	30	Sornalingam et 2016
	272.38	232.6 ± 3.0	1.170 ± 0.06	3.86×10^{-22}	2.81	3.5	10.46±0.03	13	Sornalingam et 2016
	288.38	229.6 ± 3.0	1.255 ± 0.06	3.81×10^{-22}	2.81	3.5	10.38±0.02	13	Sornalingam et 2016
2	296.40	244.4 ± 3.0	1.21 ± 0.01	4.06×10^{-22}	3.67-4.20	3.8	10.40	4.7-19	Sornalingam et 2016
A	228.29	199.5 ± 3.0	1.143 ± 0.06	3.31×10^{-22}	3.32		9.6-10.02	120	Ying et al., 20
P	150.22	154.5 ± 3.0	0.971 ± 0.06	2.57×10^{-22}	3.31	3.39	10.16	610	Pubchem

- *log* K_{ow} values of BPA and 4*t*BP were taken from PubChem. The molar mass, molar volume and molar density were calculated using ChemSketch software.

Table 2. Kinetic parameters calculated from the PSO and Weber-Morris kinetic models for the sorption of EDCs on fBC at 25 °C.

	PSO at 25 ± 0.5 °C			Initial linear portion			2nd linear portion			3rd linear portion		
EDC	q_s (μg g^{-1})	K_2 (μg g^{-1} min^{-1})	r^2	C_1 (μg g^{-1})	K_{i1} (μg g^{-1} min$^{-0.5}$)	r^2	C_2 (μg g^{-1})	K_{i2} (μg g^{-1} min$^{-0.5}$)	r^2	C_3 (μg g^{-1})	K_{i3} (μg g^{-1} min$^{-0.5}$)	r^2
E1	7642±476	2.56E-7±5.7E-8	0.969	592±402	167±23	0.930	1735±192	131±6	0.996	5959±261	25±6	0.905
E2	5439±306	1.05E-6±3.03E7	0.933	1646±266	108±15	0.926	3002±99	51±3	0.994	4355±186	18±4	0.905
E3	4403±409	1.88E-7±5.3E-8	0.979	685±386	96±22	0.816	170±251	66±7	0.969	2629±171	11±4	1.000
EE2	5468±188	8.33E-7±1.36E-7	0.978	1079±61	119±4	0.996	2040±239	77±7	0.984	4995±64	8±1	0.937
BPA	4749±188	4.82E-7±7.67E-8	0.984	71±754	110±4	0.994	1176±288	63±8	0.965	3812±12	9±1	1.000
4*t*BP	4431±198	5.52E-7±1.02E-7	0.978	32±2705	105±15	0.919	960±269	62±7	0.960	2276±20	34±0	1.000

Table 3. ΔG^{o} values calculated from water dissociation constant (K_{aw}) at 25 ^{o}C.

EDC	Temperature (K)	pK_{a1}	$K_{a1}\times 1$ 0^{-11}	$K_{aw}\times 1$ 0^{-14}	$ln\ K_{aw}$	RT ln K_{aw} (J mol^{-1})	RT ln K_{aw} (kJ mol^{-1})	RT ln K_{a1} (kJ mol^{-1})	$\Delta G^{0}_{H^{+}_{exch}1}$ (kJ mol^{-1})
E1	298	10.34	4.58	1.01	-32.23	-79858	-79.86	-59.00	-20.86
E2	298	10.46	3.47	1.01	-32.23	-79858	-79.86	-59.67	-20.19
E3	298	10.38	4.17	1.01	-32.23	-79858	-79.86	-59.22	-20.64
EE2	298	10.40	3.98	1.01	-32.23	-79858	-79.86	-59.33	-20.54
BPA	298	9.80	15.85	1.01	-32.23	-79858	-79.86	-55.91	-23.95
4*t*BP	298	10.16	6.92	1.01	-32.23	-79858	-79.86	-58.00	-21.86

- K_{aw} values were taken from http://www.chemguide.co.uk/physical/acidbaseeqia/kw.html
- R =8.314 (J K^{-1} mol^{-1}), $\Delta G^{0}_{H^{+}_{exch}1} = -RT\ ln(K_{a1}/\ K_{aw})$

Table 4. EDC removal from synthetic wastewater with different dosages of fBC at 46 h, 50 h and 64 h.

Initial conc.	Dosage	46 h		50 h		64 h	
(μg L^{-1})	(mg L^{-1})	Residual conc. (μg L^{-1})	Removal (%)	Residual conc. (μg L^{-1})	Removal (%)	Residual conc. (μg L^{-1})	Removal (%)
	110	400.0	11.9	377.1	18.2	367.0	20.4
	225	269.4	41.6	255.9	44.5	249.2	46.0
461.3	333	208.7	54.7	202.0	56.2	178.5	61.3
	445	87.5	81.0	80.8	82.5	47.1	89.8
	555	26.9	94.2	16.8	96.4	<LOD	~100
	110	419.4	13.7	392.8	19.2	352.8	35.2
	225	233.0	52.1	219.7	54.8	186.4	61.6
486.0	333	166.4	65.8	159.8	67.1	119.8	75.3
	445	39.9	91.8	<LOD	~100	<LOD	~100
	555	<LOD	~100	<LOD	~100	<LOD	~100
	110	373.3	25.2	350.2	29.8	304.5	38.9
	225	159.8	67.9	152.3	69.5	125.6	74.8
498.7	333	125.6	74.8	76.1	84.7	60.9	87.8
	445	11.4	97.7	3.8	99.2	<LOD	~100
	555	<LOD	~100	<LOD	~100	<LOD	~100
	110	418.1	15.9	385.5	22.4	371.6	25.2
	225	209.0	57.9	199.7	59.8	153.2	69.2
497.0	333	102.2	79.4	88.3	82.2	74.3	85.0
	445	4.6	99.1	4.6	99.1	<LOD	~100
	555	<LOD	~100	<LOD	~100	<LOD	~100
	110	388.2	16.7	336.5	27.8	284.7	38.9
	225	118.1	61.1	155.3	66.7	129.4	72.2
465.9	333	77.6	83.3	25.9	94.4	25.9	94.4
	445	25.9	94.4	<LOD	~100	<LOD	~100
	555	<LOD	~100	<LOD	~100	<LOD	~100
	110	258.1	43.9	230.2	50.0	209.3	54.5
	225	244.2	47	230.2	50.0	188.4	59.1
460.4	333	111.6	75	104.6	77.3	69.7	84.8
	445	27.9	93.9	6.9	98.5	<LOD	~100
	555	<LOD	~100	<LOD	~100	<LOD	~100

Highlights

- fBC removed ~100% of EDC mixture from water and wastewater.
- Sorption affinities decreased as E1 > E2 ≥ EE2 > 4*t*BP > BPA > E3.
- Sorption in wastewater was reduced by 38-50% due to sodium laryl sulphonate.
- π-π EDA interactions with H-bond formation were main sorption mechanism.